Density Functional Theory Calculations of Pressure Effects on the Structure and Vibrations of 1,1-Diamino-2,2-dinitroethene (FOX-7)

ARTICLE *in* THE JOURNAL OF PHYSICAL CHEMISTRY A · OCTOBER 2014

Impact Factor: 2.69 · DOI: 10.1021/jp508869n · Source: PubMed

3 AUTHORS, INCLUDING:

Boris B. Averkiev
Washington State University
81 PUBLICATIONS **1,190** CITATIONS

SEE PROFILE

Zbigniew Dreger
Washington State University
124 PUBLICATIONS **1,127** CITATIONS

SEE PROFILE

THE JOURNAL OF PHYSICAL CHEMISTRY A

Article

pubs.acs.org/JPCA

Density Functional Theory Calculations of Pressure Effects on the Structure and Vibrations of 1,1-Diamino-2,2-dinitroethene (FOX-7)

Boris B. Averkiev, Zbigniew A. Dreger,* and Santanu Chaudhuri

Institute for Shock Physics, Washington State University, Pullman, Washington 99164-2816, United States

ABSTRACT: Pressure effects on the Raman vibrations of an energetic crystal FOX-7 (1, 1-diamino-2, 2-dinitroethene) were examined using density functional theory (DFT) calculations. High accuracy calculations were performed with a periodic plane-wave DFT method using norm-conserving pseudopotentials. Different exchange−correlation functionals were examined for their applicability in describing the structural and vibrational experimental data. It is shown that the PBE functional with an empirical dispersion correction by Grimme, PBE-D method, reproduces best the molecular geometry, unit cell parameters, and vibrational frequencies. Assignments of intramolecular Raman active vibrations are provided. The calculated pressure dependence of Raman shifts for the intramolecular and lattice modes were found to be in good agreement with the experimental data; in particular, the calculations predicted correctly a decrease of frequencies for the NH_2 stretching modes with pressure. Also, in accord with experiments, the calculations indicated some instances of modes mixing/coupling with increasing pressure. This work demonstrates that the dispersion-corrected PBE functional can account for the structural and vibrational properties of FOX-7 crystal at ambient and high pressures.

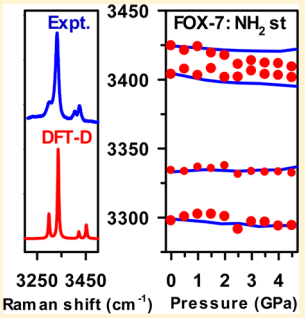

I. INTRODUCTION

1,1-Diamino-2,2-dinitroethene (FOX-7 or DADNE) is an energetic crystal with excellent performance and low initiation sensitivity.[1−3] Because of these attractive characteristics, there has been considerable interest in identifying microscopic properties of FOX-7 under various external conditions. Of particular interest are vibrational properties at high pressure, as they are critical for understanding the strength and stability of molecular and intermolecular bonding, molecular interactions, vibrational coupling, and, thus, the reactive behavior under shock wave compression. To gain insight into these characteristics, a detailed knowledge of the molecular response under compression is required.

As shown previously for PETN (pentaerythritol tetranitrate)[4−7] and RDX (cyclotrimethylene trinitramine),[8−16] progress in understanding molecular processes in energetic crystals under extreme conditions can be achieved through a concerted experimental and computational approach. In the case of FOX-7, this progress has been hampered by a lack of comprehensive, experimental vibrational data, and deficiency in vibrational assignments. However, recent measurements of Raman spectra on single crystals over a broad range of frequencies and pressures[17,18] provided detailed results that can be used for evaluating computational approaches. Here, we use density functional theory (DFT) calculations of the structural and vibrational properties of FOX-7 under static compression to complement the experimental data and to advance the understanding of FOX-7 behavior under high pressures.

At ambient conditions, FOX-7 $[C_2(NH_2NO_2)_2]$ crystallizes in a monoclinic structure with a space group of $P2_1/n$. The molecules in the crystal are arranged "head-to-tail" to form wave-shaped layers with an extensive network of hydrogen bonding in the layers and weak van der Waals forces between the layers (see Figure 1). Single crystal X-ray diffraction studies have demonstrated that the room temperature structure (α-FOX-7) is unstable at high temperatures and transforms to two other polymorphs, β and γ.[19,20]

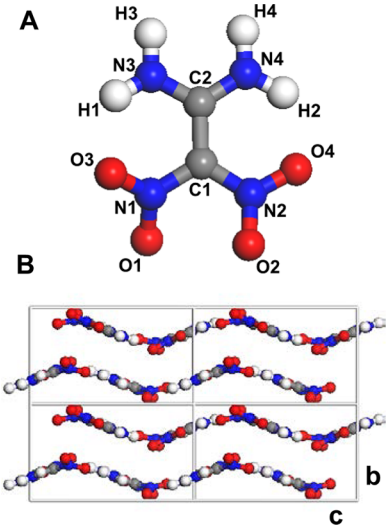

Figure 1. Molecular and crystal structures of FOX-7 at ambient conditions. (A) Molecule with labeled atoms to assist with the bonding designation. (B) Projection of the crystal structure on the (011) plane, showing arrangement of wave-shaped layers; crystal unit cells are represented by gray lines.

Received: September 2, 2014
Revised: October 3, 2014
Published: October 7, 2014

   dx.doi.org/10.1021/jp508869n | J. Phys. Chem. A 2014, 118, 10002−10010

Table 1. Calculated and Experimental Volumes and Unit Cell Parameters of FOX-7 at Ambient Pressure[a]

	LDA CA-PZ	GGA PBE	GGA PBE-D	GGA PBE-D[b]	expt[c]	error[d] %
V, Å	466.83	664.35	519.03	515.45	515.89	0.6
a, Å	6.77	7.24	7.03	6.99	6.941	1.2
b, Å	6.22	7.80	6.52	6.52	6.569	−0.7
c, Å	11.09	11.77	11.33	11.31	11.315	0.1
β, deg	90.68	91.96	91.02	91.23	90.55	0.5

[a]Calculated results are at T = O K. [b]ref 28. [c]ref 1 (results obtained at T = 173 K). [d]Error was obtained from the formula: (Result (column 3) − Result (column 5))/Result (column 5).

The structural stability of α-FOX-7 was also examined under high pressure using X-ray powder diffraction[21] and vibrational spectroscopy.[17,18,21−23] The X-ray studies provided approximate changes in the unit cell parameters up to 3.86 GPa, whereas the vibrational studies suggested phase transitions at several different pressures. In particular, recent Raman studies on single crystals revealed spectral changes at 2 and 4.5 GPa. They were tentatively attributed to minor changes in the molecules conformation at 2 GPa and a significant transformation in the crystal structure at 4.5 GPa.[17,18] This work also provided pressure dependencies of all Raman active modes and demonstrated a considerable coupling between various modes with increasing pressure.

There exist several previous computational studies to examine pressure effects on FOX-7 crystal structure, using density functional theory (DFT).[24−28] Both the local density approximation (LDA) and the generalized gradient approximation (GGA) were used for the exchange−correlation potentials.[24,25] The calculated ambient and high pressure unit cell parameters were clearly either underestimated by LDA or overestimated by GGA, due to the insufficient treatment of van der Waals interactions by these standard approximations. Recently, it was shown that the use of DFT methods with empirical dispersion correction addresses these deficiencies and significantly improves the agreement between the calculated and experimental unit cell parameters.[26−28] In contrast to the crystal structure calculations of FOX-7, there have been few theoretical studies of vibrational properties.[21,28,29] Among these, only one study reported crystal calculations;[28] the other two were for the gas phase or single molecule. The vibrational calculations for the crystal were performed using DFT method, with dispersion correction (DFT-D) to account for the weak interactions. The pressure dependence of selected IR frequencies was obtained up to 10 GPa, using the Vanderbilt ultrasoft pseudopotential. However, there was no attempt to evaluate this approach using experimental IR data.

Because Raman spectroscopy is a valuable tool for probing molecular changes in energetic crystals under static[5,7,8,18] and dynamic[6,9] compression, there is an important need for better characterization of the Raman spectra. Here, we provide a full assignment of Raman active vibrations and calculate pressure effects on the Raman spectra of FOX-7 crystal. We applied primarily the DFT method with dispersion correction as in ref 28, but we used a norm-conserving pseudopotential, which is required for accurate Raman intensity calculations. However, we also used the standard DFT approximations to examine their applicability for describing the structural and vibrational properties. The calculated results are evaluated by comparison with experimental data.

The rest of the paper is organized as follows. The computational methods are described in section II. The molecular, crystal, and vibrational structures of FOX-7 at ambient pressure are presented in section III. In section IV, we present and discuss the pressure effects. Finally, the main findings are briefly summarized in section V.

II. COMPUTATIONAL METHODS

The calculations were performed using the periodic plane-wave pseudopotential DFT method implemented in the CASTEP program.[30] The generalized gradient approximation (GGA) with the Perdew−Burke−Ernzerhof (PBE)[31] parametrization and plane-wave basis set with norm-conserving pseudopotential and energy cutoff of 830 eV were used. The empirical dispersion correction by Grimme[32] was used to take into account weak nonbonded interactions. For comparison with experimental results, we also used local density approximation (LDA) of Ceperley and Adler[33] parametrized by Perdew and Zunger (CA-PZ).[34] The Brillouin zone of the reciprocal space of FOX-7 crystal was sampled by Monkhorst−Pack grid:[35] 2 × 2 × 1 k points for structure at ambient pressure up to 2 × 3 × 1 k points for structure at 20 GPa to maintain a minimum k-point separation of 0.07 Å^{-1}. The Broyden−Fletcher−Goldfarb−Shanno (BFGS) algorithm[36] was utilized to optimize the unit cell parameters and atomic coordinates simultaneously, while maintaining the same crystal structure symmetry. The convergence criteria for geometry optimization were the following: maximum change in system energy of 5 × 10^{-6} eV/atom, maximum force of 0.01 eV/Å, maximum stress of 0.02 GPa, and maximum displacement of 5 × 10^{-6} Å. Vibrational properties and Raman spectra were calculated at the Γ point using the finite displacement approach.[37]

Changes in the character of vibrations due to high pressure were analyzed by comparing their normal modes. The normal modes form an orthonormal basis in 3N dimensional vector space, where N is the number of atoms. Correspondingly, each 3N normal modes at high pressure (HP) can be expressed as a linear combination of initial 3N normal modes at ambient pressure (amb). In the simplest case, if the character of vibration does not change with pressure, the normal mode of vibration, ν_i^{HP}, is represented by one ambient vibration $\nu_i^{HP} = \nu_i^{amb}$. In more complex cases, several vibrations can mix under high pressure, and they can be expressed as a linear combination of two or more ambient vibrations.

$$\nu_i^{HP} = C_{i1}\nu_1^{amb} + C_{i2}\nu_2^{amb} + C_{i3}\nu_3^{amb} + \cdots$$

The sum of squares of coefficients must be equal to unity. However, the square of each coefficient, C_{ij}^2, represents the contribution of the character of ambient vibration ν_j^{amb} into the character of the vibration under high pressure.

The intensities of molecular vibrations (I_i) were obtained from their activities (S_i) using the following relationship:[38]

Table 2. Geometrical Parameters of FOX-7 Molecule in the Crystal at Ambient Pressure[a]

					errors		
	GGA PBE-D	GGA PBE	LDA CA-PZ	expt[b]	GGA PBE-D	GGA PBE	LDA CA-PZ
C1−C2	1.463	1.463	1.453	1.456	0.01	0.01	0.00
C1−N1	1.417	1.420	1.396	1.398	0.02	0.02	0.00
C1−N2	1.430	1.433	1.405	1.427	0.00	0.01	−0.02
N1−O1	1.259	1.258	1.252	1.252	0.01	0.01	0.00
N1−O3	1.263	1.262	1.253	1.249	0.01	0.01	0.00
N2−O2	1.254	1.251	1.249	1.242	0.01	0.01	0.01
N2−O4	1.257	1.260	1.247	1.242	0.01	0.02	0.01
C2−N3	1.334	1.337	1.321	1.319	0.02	0.02	0.00
C2−N4	1.340	1.342	1.326	1.325	0.02	0.02	0.00
C2−C1−N1−O3	6.3	9.5	5.1	5.8	0.5	3.7	−0.7
C2−C1−N2−O4	31.8	27.8	30.2	34.3	−2.4	−6.5	−4.1

[a]Bonds length in Å and angles in degrees. [b]ref 1.

Table 3. Geometrical Parameters of Hydrogen Bonds in FOX-7 Crystal at Ambient Pressure

H-bond	GGA PBE-D				GGA PBE	LDA CA-PZ	expt[a]	GGA PBE-D	GGA PBE	LDA CA-PZ
	N−H (Å)	H···O (Å)	∠ NHO (deg)	N···O (Å)	N···O (Å)	N···O (Å)	N···O (Å)	errors for N···O distance (Å)		
N3−H1···O3	1.021	1.867	127.21	2.615	2.604	2.575	2.608	0.01	0.00	−0.03
N4−H2···O4	1.020	1.891	126.11	2.625	2.610	2.575	2.636	−0.01	−0.03	−0.06
N3−H3···O1	1.026	2.006	154.75	2.966	3.002	2.824	3.000	−0.03	0.00	−0.18
N4−H4···O1	1.024	2.278	143.51	3.160	3.051	3.002	3.191	−0.03	−0.14	−0.19
N4−H4···O2	1.024	2.002	142.31	2.881	2.966	2.748	2.900	−0.02	0.07	−0.15
N3−H1···O2	1.021	2.226	137.19	3.055	3.175	2.872	3.009	0.05	0.17	−0.14
N3−H3···O4	1.026	2.464	112.58	3.010	3.091	2.851	3.012	0.00	0.08	−0.16
N4−H2···O3	1.020	2.310	130.81	3.076	3.323	2.878	3.026	0.05	0.30	−0.15

Atom labeling as in Figure 1. [a]ref 1.

$$I_i = f\frac{(\nu_0 - \nu_i)^4 S_i}{\nu_i\left[1 - \exp\left(-\frac{hc\nu_i}{kT}\right)\right]}$$

Where ν_0 is the laser excitation frequency, ν_i is the vibrational wavenumber of the ith normal mode, h, c, and k are fundamental constants, and f is a suitably chosen common scaling factor. In our calculations, we used ν_0 = 532 nm = 18797 cm^{-1} and T = 293 K.

III. AMBIENT PRESSURE

A. Crystal and Molecular Structure. Before calculating the crystal Raman frequencies, we first examined the ability of the computational approaches for reproducing the experimental molecular packing and molecular geometry. The calculated and experimental unit cell parameters are compared in Table 1. As expected, the standard GGA and LDA methods generated large errors due to the underestimation (GGA) or overestimation (LDA) of the intermolecular interactions. The errors are more pronounced in the crystallographic b-direction, where the crystal is bonded by the van der Waals forces. On the other hand, the PBE-D method, with norm-conserving pseudopotential and ultrasoft pseudopotential yield similar results and reproduce well the experimental unit cell. The calculated unit cell volume in this work is 519.03 $Å^3$, which is less than 1% larger than the experimental value of 515.89 $Å^3$. Furthermore, the calculated lattice parameters: a, b, c, and β are 7.03 Å, 6.52 Å, 11.33 Å, and 91.02°, and their relative errors are 1.2, −0.7, 0.1, and 0.5%, respectively, as shown in Table 1.

The geometrical parameters of the molecules in the crystal are presented in Table 2.

As expected, the empirical dispersion correction does not influence bond distances, but it affects calculated torsion angles. The experimental data and calculations show that the molecule geometry in the crystal deviates significantly from the C_2 symmetry in the gas phase. This deviation is caused by intermolecular interactions and is manifested by the different orientation of NO_2 groups. The calculated torsion angles C2−C1−N1−O3 and C2−C1−N2−O4 are 6.3 and 31.8°, respectively, and the bond lengths of C1−N1 and C1−N2 are 1.417 and 1.430 Å. We also calculated distance between the overlapping molecules from neighboring layers and the angle between planes of molecules to be 3.05 Å and 37.5°, respectively. All these values are in good agreement with the experimental structure.[1]

There are two intramolecular hydrogen bonds and six different types of intermolecular hydrogen bonds in the FOX-7 crystal. Their geometrical parameters are given in Table 3. The comparison of calculated N···O distances with experimental data demonstrates clearly the importance of dispersion correction. Both LDA and GGA standard methods either underestimate or overestimate the bond length. The mean unsigned errors for N···O distances are equal to 0.03, 0.10, and 0.13 Å for PBE-D, PBE, and LDA methods, respectively.

B. Vibrational Properties. In FOX-7, there are a total of 165 optical modes. For the space group $P2_1/n$ (C_{2h}), a group-theoretical analysis gives the following decomposition of vibrational representation into irreducible components: Γ_{inter} = $36A_g + 36B_g + 36A_u + 36B_u$ (internal) and $\Gamma_{latt} = 6A_g + 6B_g + 5A_u + 4B_u$ (lattice). From these, the modes with inversion symmetry, A_g and B_g, are Raman active. Thus, there are 36 internal and 6 lattice Raman vibrations of each symmetry.

dx.doi.org/10.1021/jp508869n | J. Phys. Chem. A 2014, 118, 10002−10010

Table 4. Calculated and Experimental Frequencies for NH_2 Stretching Vibrations of Ag Symmetry in FOX-7 Crystal

frequency (cm^{-1})				error (cm^{-1})		
GGA PBE-D	GGA PBE	LDA CA-PZ	expt[a]	GGA PBE-D	GGA PBE	LDA CA-PZ
3293	3291	3163	3299	−6	−8	−136
3334	3319	3207	3333	1	−14	−126
3424	3427	3300	3405	19	22	−105
3450	3429	3311	3425	26	4	−114

[a]ref 18.

To test the ability of the computational methods for reproducing the experimental data, we examined the region of NH_2 stretching modes. The results of the examination are listed in Table 4. We note that the LDA method is not reliable for FOX-7 because it produces values that are significantly different from the experiments. On the other hand, both GGA methods provide good agreement with the experimental data. However, we used the PBE-D approach in further calculations because it reproduces the molecular geometry and overall crystal structures with greater accuracy. The calculated and experimental Raman spectra are compared in Figure 2, in the frequency range from 200 to 3500 cm^{-1}. The calculated spectra were simulated by using the Lorentzian broadening of 6 cm^{-1} to the computed frequencies. The good similarity between the major features of the calculated and the experimental spectra confirms that the PBE-D method reproduces well the experimental results.

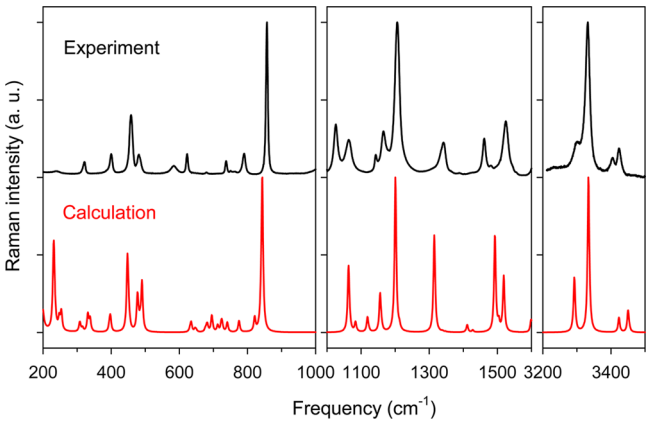

Figure 2. Calculated and experimental Raman spectra of FOX-7. The intensity of the strongest peak in each panel was normalized to the same value.

In Table 5, we list the characteristics of the calculated internal vibrational modes of FOX-7, including frequencies, symmetry and vibrational assignments, and pressure dependencies. The calculations were performed using the DFT-D method. An examination of this table indicates that frequencies of A_g and B_g vibrations are quite close, and usually the A_g vibration has a higher Raman intensity than the corresponding B_g vibration. Because of this, some B_g modes are buried under the A_g modes, which simplifies the spectral appearance. However, in the low-frequency region the intensities of A_g and B_g vibrations are comparable, which results in a complex spectra. It can also be seen that most of modes are a combination of different vibrations delocalized over the molecule. Furthermore, examination of the table indicates that the calculated and experimental frequencies generally differ by only several wavenumbers. The one exception is mode 21 (NH_2 rocking), which differs by 39 cm^{-1} from the experimental value.

As previously mentioned, the molecule geometry in the crystal deviates significantly from the C_2 symmetry attained in the gas phase. However, most of the molecular vibrations in the crystal are quite similar to single molecule vibrations in the gas phase; thus, they can also be classified as symmetric (A) and antisymmetric (B) in terms of the C_2 point group.

We also note that the modes corresponding to similar types of internal vibrations are located in the same parts of the spectra. The lower frequency modes, from ∼120 to 500 cm^{-1}, correspond to variety of skeletal deformations of the molecule. The diverse NH_2 twisting and wagging vibrations belong to the frequency range from 620 to 700 cm^{-1}. The higher frequencies, from 720 to 1430 cm^{-1}, have rather complicated character and consist of NO_2 scissoring and stretching modes, C−C and C−N stretching modes, and N−C−N rocking. All these vibrations are mixed with NH_2 vibrations. The lower-frequency modes in this group, 720 to 860 cm^{-1}, are combined with out-of-plane twisting NH_2 vibrations, whereas higher-frequency modes in this group, 1000 to 1430 cm^{-1}, are combined with in-plane scissoring or rocking NH_2 vibrations. The vibrations between 1490 and 1630 cm^{-1} correspond to NH_2 scissoring and C−C stretching or rocking. Finally, the high-frequency vibrations, between 3200 and 3500 cm^{-1} correspond to NH_2 stretching vibrations.

The calculated and experimental frequencies in the lowest frequency range are presented in Table 6. The calculations were performed using the DFT-D method. This range is attributed to vibrations of the crystal lattice. In FOX-7, there are 12 such modes. We noticed that these modes are not well-separated from the low-frequency molecular vibrations. Examination of the atomic motions reveals that in the range of 100−200 cm^{-1}, the rotational lattice vibrations mix with low-frequency molecular vibrations.

IV. HYDROSTATIC PRESSURE

A. Crystal and Molecular Structure. As previously indicted, FOX-7 likely undergoes two phase transitions at 2 and 4.5 GPa, as revealed by the Raman spectroscopy.[17,18] The structures of these phases are unknown. However, from Raman spectra changes, it is inferred that structural changes at 2 GPa are minimal as opposed to changes at 4.5 GPa.[18] Therefore, in this work, the pressure effects were calculated only up to 4.5 GPa. Furthermore, we maintained the same ambient space group at all pressures, regardless of the possible molecular change at 2 GPa, as deduced from the Raman experiments.

In Figure 3, we present pressure effects on the unit cell volume and parameters. The results are compared with previous calculations[28] and the powder diffraction X-ray data.[21] It can be seen that the type of pseudopotential practically does not affect the calculation results as long as

dx.doi.org/10.1021/jp508869n | J. Phys. Chem. A 2014, 118, 10002−10010

Table 5. Characteristics of Intramolecular Vibrational Modes in FOX-7 Crystal at Ambient Pressure and Pressure Dependencies of Frequencies up to 4.5 GPa[a]

	A_g	B_g	expt[c]	vibrational assignment	mol.[d] sym.	dν/dp calcd	dν/dp expt[c]
1	123 (40)[b]	114 (39)		NO_2 twist, C−$(NH_2)_2$ twist, in phase	A	8.6	
2	194 (48)	185 (11)		NO_2 twist, C−$(NH_2)_2$ wag	B	5.5	
3	233 (15)	231 (34)		NO_2 twist, C−$(NH_2)_2$ twist, opposite	A	6.4	
4	253 (9)	247 (6)	246	C−C−$(NO_2)_2$ umb	B	6.4	7.7
5	316 (2)	308 (5)	318	NO_2 rock, NH_2 twist	A	3.1	6.9
6	331 (9)	338 (6)		C(2)N_2 and C(1)N_2 rock	B	3.2	
7	397 (7)	395 (3)	400	C(2)N_2 and NO_2 rock, opposite	B	6.4	4.9
8	448 (38)	452 (4)	457	C(2)N_2 and NO_2 rock, in phase	B	3.0	6.2
9	477 (17)	480 (2)	472	skeletal breathe	A	2.8	7.0
10	490 (24)	485 (3)	481	skeletal breathe	A	1.2	9.7
11	634 (5)	631 (1)	622	NH_2 wagging	A	2.4	3.9
12	646 (2)	649 (1)		NH_2 wagging and rocking		4.2	
13	676 (1)	679 (0)		C(2)C(1)N_2 umb, NH_2 wagging	B	2.5	
14	681 (2)	682 (2)		NH_2 twisting	A	5.0	
15	695 (8)	712 (3)		NH_2 wagging	B	15.0	
16	723 (4)	726 (3)	737	CNO_2 umb, NH_2 twist	A	1.9	1.5
17	741 (3)	740 (2)	749	CNO_2 umb, NH_2 twist	B	−0.3	0.9
18	775 (2)	775 (4)	789	ONCNO rock, NO_2 scissor, NH_2 twist	B	1.6	−1.8
19	821 (6)	821 (1)		NH_2 twist	B	5.0	
20	843 (79)	839 (2)	856	NO_2 scissor, C−C st, NH_2 twist		3.1	2.0
21	1063 (42)	1067 (3)	1024	NH_2 rock	A	1.7	0.6
22	1084 (5)	1083 (1)	1070	NH_2 rock	B	4.0	4.8
23	1119 (9)	1123 (1)	1142	NH_2 rock, C−NO_2 st(asym), NO_2 st (sym)	B	3.6	4.3
24	1156 (25)	1161 (1)	1165	NH_2 rock, C−C st	A	3.9	0.6
25	1201 (100)	1213 (3)	1208	C−NO_2 st (asym), NH_2 scissor	B	6.2	2.6
26	1315 (62)	1318 (2)	1311	C−NO_2 st (sym), NH_2 rock	A	7.8	2.4
27	1339 (0)	1348 (0)	1343	NO_2 st (asym), NH_2 scissor	B	5.1	4.9
28	1411 (5)	1428 (1)	1386	C−C st, NH_2 rock, NO_2 st (asym)	A	2.7	0.7
29	1493 (63)	1504 (5)	1506	NH_2 scissor, C−C st, in phase	A	4.9	1.4
30	1519 (33)	1518 (3)	1528	NH_2 scissor, C−C rock, opposite	B	3.8	1.9
31	1599 (8)	1609 (1)	1606	NH_2 scissor, C−C st, opposite	A	3.9	1.7
32	1624 (8)	1626 (0)	1630	NH_2 scissor, C−C rock, in phase	B	2.8	4.5
33	3293 (31)	3296 (1)	3299	NH_2 st (sym)	B	−2.4	−1.6
34	3334 (90)	3339 (2)	3333	NH_2 st (sym)	A	−0.6	2.2
35	3424 (8)	3425 (0)	3405	NH_2 st (asym)	B	−0.6	−2.6
36	3450 (13)	3455 (1)	3425	NH_2 st (asym)	A	−3.1	−2.0

[a]The calculations were performed using the DFT-D method. [b]Numbers in parentheses denote relative intensities of modes with respect to the intensity of mode 25. [c]ref 18. [d]This column represents symmetry of molecular vibrations in terms of molecular symmetries; dν/dp are the frequency slopes at ambient pressure; twist = twisting, rock = rocking, wag = wagging, scissor = scissoring, umb = umbrella, st = stretching, sym = symmetric, asym = asymmetric.

dispersion corrections are present; both calculations are in a good agreement with the experimental data. In particular, compressibility along the b-direction is higher than along the a- and c-directions, consistent with the weaker interactions between the layers than within the layers.

In Figure 4, we present pressure-dependent changes in selected molecular parameters. We found that among all the molecular bonds in FOX-7, the C1−N1 and C1−N2 bonds are most affected by pressure. At 4.5 GPa, they are shortened by 0.014 and 0.013 Å, respectively. The C2−N3, C2−N4, and C1−C2 bonds are reduced by 0.007, 0.008, and 0.007 Å. However, the lengths of N−O bonds practically do not depend on pressure. Furthermore, the molecules become less planar; the torsion angle C2−C1−N1−O3 decreases from 6.3 to 3.4°, but the torsion angle C2−C1−N2−O4 increases from 31.8 to 35.0°. Importantly, the distance between overlapping molecules from neighboring hydrogen-bonded layers decreases considerably under the pressure. It changes from 3.05 Å at ambient pressure to 2.68 Å at 4.5 GPa. Additionally, the layers become less planar. The angle between planes of molecules in a layer increases from 37.5° up to 43.3°. Because there are no experimental data on structural changes in FOX-7 under high pressure, except changes in the unit cell parameters, these results cannot be validated. Hopefully, the results obtained here will stimulate further experimental work.

B. Vibrational Properties. Figure 5 shows the pressure dependence of some calculated internal modes as compared with the experimental results. To facilitate comparison of the pressure dependence, the calculated frequencies at all pressures are shifted by the same amount so that the calculated and experimental values match at ambient pressure. As seen in Figure 5 and Table 5, most vibrational frequencies increase with increasing pressure, except the NH_2 stretching vibrations and modes 17 and 18, which have contribution from the NH_2

dx.doi.org/10.1021/jp508869n | J. Phys. Chem. A 2014, 118, 10002−10010

Table 6. Frequencies of Lattice Modes of FOX-7 at Ambient Pressure[a]

	frequency (cm^{-1})		
		symmetry	expt[a]
1	30	A_g	25
2	44	A_g	46
3	61	A_g	54
4	75	B_g	63
5	80	B_g	77
6	94	B_g	90
7	96	A_g	98
8	103	A_g	98
9	104	B_g	98
10	117	A_g	107
11	124	B_g	107
12	128	B_g	139

[a]The calculations were performed using the DFT-D method. [b]ref 18.

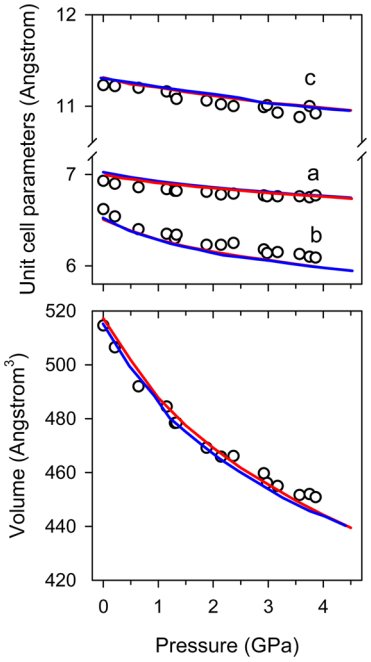

Figure 3. Pressure-induced changes in the unit cell volume and parameters up to 4.5 GPa. Lines denote calculated results: the red lines represent this work (PBE-D with norm-conserving pseudopotential) and the blue lines represent the results from ref 28. (PBE-D with ultrasoft pseudopotential). Open circles denote experimental data from ref 21.

twisting vibrations. Though the calculated and experimental pressure coefficients, $d\nu/dp$, at ambient pressure differ considerably in many cases (see Table 5), likely due to numerical fluctuations in the calculations, the pressure dependencies of calculated frequencies over the pressure range to 4.5 GPa are in good agreement with the experimental data (see Figure 5). In particular, the calculations predict correctly the "red shift" observed experimentally for the NH_2 stretching vibrations. This behavior was attributed to the strengthening of hydrogen bonding in FOX-7 under pressure.[18,22]

As we have already mentioned, the experimental Raman spectra showed several changes around 2 GPa, which were

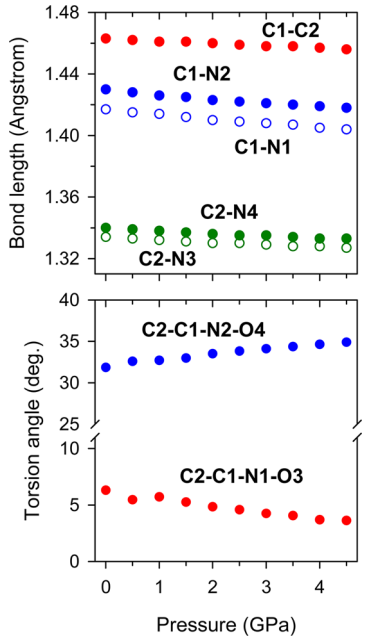

Figure 4. Effect of pressure on the parameters of FOX-7 molecule in the crystal environment. The labeling of atoms is presented in Figure 1.

attributed to changes in the molecular conformation.[18] The spectral changes at this pressure included occurrence of new peaks at 151 and 607 cm^{-1} and disappearance of a peak at 499 cm^{-1}. In addition, several peaks showed change in Raman shift slope at the transition. None of these features were reproduced in the calculated spectra, likely due to the subtle nature of this transition.

In addition to frequency changes, we also observed instances of changing the character of molecular vibrations; a close in frequency modes mixed with each other. We quantitatively analyzed the change of the character of these vibrations using their normal modes' coordinates, as was described in section II: Computational Methods. In the low frequency range, the mixing concerned modes 1 and 2. Both of these vibrations involve twisting of NO_2 groups and vibration (twisting for 1 or wagging for 2) of C-$(NH_2)_2$ group. Also, as it was mentioned before, these modes are mixed with lattice rotational vibrations. At higher pressure these modes have rather complex vibrational character that includes all three types of vibrations (NO_2 groups, C-$(NH_2)_2$ group, and molecular rotation) and cannot be classified as having A or B molecular symmetry anymore. The modes 9 and 10 (see, Table 5), corresponding to in-plane vibrations, also start mixing when pressure increases. They already had very similar character and frequencies (477 and 490 cm^{-1}) at ambient pressure. They both can be described as molecular breathing, but they have a different contribution of stretching shift (stretching of all C−N bonds) and rocking vibrations of NO_2 and NH_2 groups. With increasing pressure, these contributions were changing.

More complex behavior was observed for the next five modes with frequencies between 600 and 700 cm^{-1}. All these modes correspond to out-of-plane twisting, wagging, and rocking vibrations of NH_2 groups. They have similar character, and under pressure, the character of each vibration can be described as a combination of their ambient pressure vibrations. Furthermore, the last mode in this group, 15, crossed modes 16 and 17 from the next group at about 2 GPa. At higher

dx.doi.org/10.1021/jp508869n | J. Phys. Chem. A 2014, 118, 10002−10010

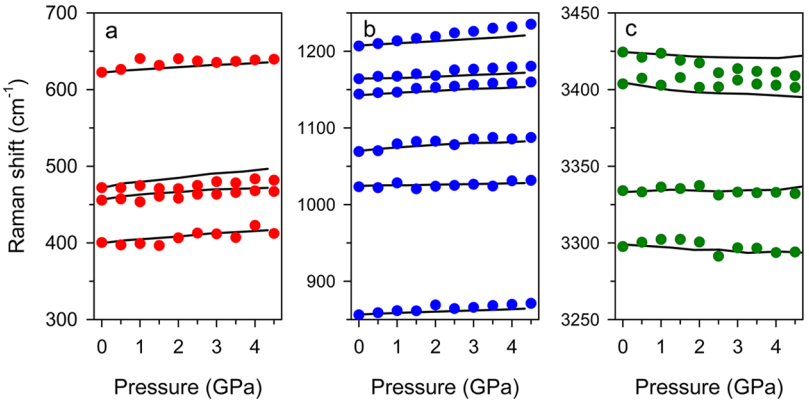

Figure 5. Pressure-induced frequency shift of selected internal modes: (a) in-plane molecular vibrations that consist of skeletal deformation, (b) in-plane molecular vibrations that consist of NH_2 rocking or scissoring and skeletal deformation, and (c) N−H stretching modes under pressure. Symbols represent the calculations, whereas solid lines represent the experiment (ref 18). The calculated frequencies at all pressures are shifted by the same amount so that the calculated values and the experimental values match at ambient pressure.

pressures, the calculated modes should be considered as a mixture of modes 15, 16, and 17. In the Raman spectra (Figure 2), all these modes are represented by a dense set of small peaks in the range 620−750 cm^{-1}.

The behavior of the rest of internal modes was fairly straightforward; with a pressure increase, the frequencies gradually increased but preserved the character of the atomic movements. Exceptions from this were two pairs of modes: 19 and 20, and 26 and 27, with more complex behavior. The mode 19 represents a pure NH_2 twisting vibration, whereas mode 20 is a combination of NO_2 scissoring, C−C stretching, and NH_2 twisting vibrations. These modes are separated by ∼20 cm^{-1}, at ambient pressure. With increasing pressure, the vibrational character of both modes is gradually mixing; the mode 19 includes more NO_2 scissoring vibrations, and the mode 20 includes less. Despite the structural change at 4.5 GPa,[18,21] we calculated crystal structure and frequencies of these modes above 4.5 GPa, assuming the same space group. A degree of mixing was quantified by coefficients (C^2), calculated from the normal modes of vibrations, which were, in turn, related to atomic shifts for vibrations (see section II). It turned out (see Figure 6) that at pressure ∼10 GPa, both modes became a 50:50 mixture of initial modes 19 and 20. At that pressure, both modes have NO_2 scissoring, C−C stretching, and NH_2 twisting vibrations. When the pressure further increases, mode 19 has more contribution from NO_2 scissoring and C−C stretching vibrations, whereas their contributions in mode 20 decreases. Lastly, at 20 GPa, mode 20 is mostly described as pure a NH_2 twisting vibration (as mode 19 at ambient pressure), although mode 19 is described as a combination of NO_2 scissoring, C−C stretching, and NH_2 twisting vibrations (as mode 20 at ambient pressure). It should be emphasized that there was no crossing of frequencies of these modes at all pressures.

Analogous behavior to that mentioned above was also observed for modes 26 and 27. Similarly to modes 19 and 20, these modes are also separated by ∼20 cm^{-1} at ambient pressure. Mode 26 consists of the C−NO_2 symmetric stretching and NH_2 rocking vibrations, whereas mode 27 consists of the NO_2 asymmetric and NH_2 scissoring vibrations. The vibrational character of these modes changed at even lower pressure in contrast to modes 19 and 20. Modes 26 and 27 exchanged fully their characters at 10 GPa. It is notable that in both cases, the minimum calculated frequency separation for both pairs, 11 cm^{-1}, occurs around 5 GPa. The predicted

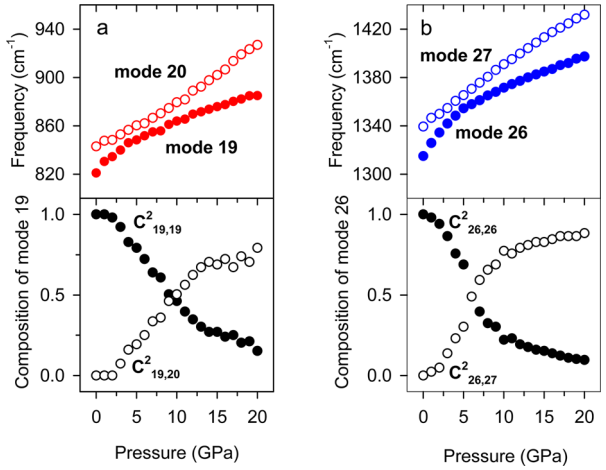

Figure 6. Illustration of pressure-induced coupling/mixing of modes: (a) Mode 19 (NH_2 twisting vibration) and mode 20 (NO_2 scissoring and NH_2 twisting vibrations) and (b) Mode 26 (C−NO_2 symmetric stretching and NH_2 rocking vibrations) and mode 27 (NO_2 asymmetric and NH_2 scissoring vibrations). Note, $C^2_{19,20}$ denotes the contribution of the character of mode 20 vibration into the mode 19 vibration. At ambient pressure, $C^2_{19,20} = 0$ (no contribution from vibration of mode 20), while $C^2_{19,19} = 1$. At higher pressure, the contribution of the character of mode 20 vibration in the mode 19 vibration increases. At about 10 GPa, $C^2_{19,20} = C^2_{19,19} = 0.5$. At 20 GPa, $C^2_{19,20} > C^2_{19,19}$; the character of mode 19 vibration has more or less the character of mode 20 at ambient pressure.".

mixing/coupling of different modes in this work is in accord with the experimental observations.[18] However, details regarding the range of pressures and type of vibrations are somewhat different in calculations than in the experimental observations. The differences are likely due to inability of the calculations to account for the phase change at 4.5 GPa. Although the molecular mechanisms for shock initiation of FOX-7 are unknown, it is often conjectured that the C−NO_2 bond homolysis could be an important step in the decomposition process.[39] Therefore, the computationally and experimentally identified coupling/mixing of the C−NO_2 vibrations with other vibrations may have implications for the shock insensitivity of FOX-7.[18]

Finally, we also calculated the effect of pressure on the lattice modes. There are a total of 12 Raman active modes, 6 A_g and 6

dx.doi.org/10.1021/jp508869n | J. Phys. Chem. A 2014, 118, 10002−10010

B_g symmetry, corresponding to lattice vibrations in FOX-7. Because we were unable to obtain reliable results using a finite displacement method due to numerical fluctuations, we repeated the calculations with a linear response method for PBE functional. The calculated results are compared with the experimental data in Figure 7 and listed in Table 6. It should be

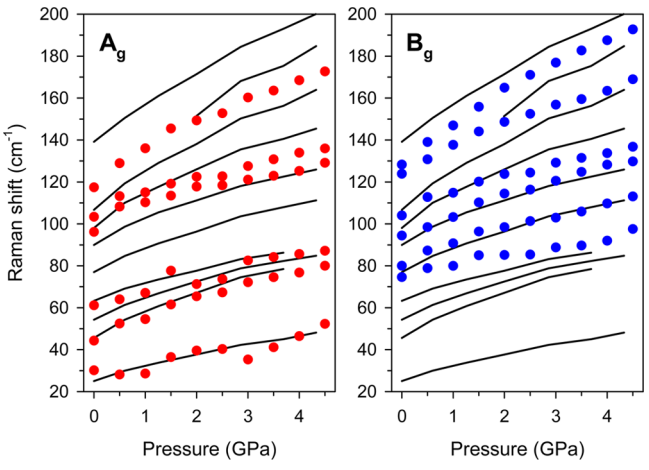

Figure 7. Pressure-induced shift of lattice modes frequency; A_g and B_g symmetries. Symbols represent the calculated results, whereas solid lines represent the experimental data (ref 18). Note that the experiments could not distinguish between A_g and B_g symmetries. Hence, the solid lines are the same in both graphs and represent the total number of detected lattice modes.

mentioned that the calculated lattice modes indicated mixing with the low-frequency internal vibrations (i.e., NO2 twisting, and $C-(NH_2)_2$ twisting and wagging). Despite this complexity, the examination of Figure 7 indicates that the calculated shifts of lattice modes reproduce the general trends observed in the experimental data.

V. SUMMARY AND CONCLUSIONS

We carried out DFT calculations to examine the pressure effects on structural and vibrational properties of the energetic crystal of FOX-7. We have provided for the first time the vibrational and symmetry assignments of internal and lattice Raman active modes. We demonstrated that GGA with PBE functional and empirical dispersion correction by Grimme[32] can reproduce well the pressure-induced changes in the unit cell parameters and the vibrational frequencies of the Raman spectra. We have also calculated changes in the molecular bonding to stimulate future experiments.

In accord with experiments, the calculations predicted a decrease of frequencies for the NH_2 stretching modes and mixing/coupling of several modes, in particular the $C-NO_2$, with increasing pressure. The complexity of mixing of character of modes and exchange of character of some modes are documented. Combination of experiments and theoretical assignments of such anomalous changes in vibrations and bonding character with pressure are important aspects of the FOX-7 insensitivity under high pressure conditions. The present work demonstrates that the DFT method with dispersion correction is a good complement to the experiments and helps in quantifying the molecular processes in FOX-7 under high pressure

AUTHOR INFORMATION

Corresponding Author

*E-mail: dreger@wsu.edu. Phone: 509-335-4233.

Notes

The authors declare no competing financial interest.

ACKNOWLEDGMENTS

We thank Prof. Y. M. Gupta for comments on this manuscript and many valuable discussions. This work was supported by DOE/NNSA Grant DE-NA0000970 and ONR Grant N000014-12-1-0555.

REFERENCES

(1) Bemm, U.; Ostmark, H. 1,1-Diamino-2,2-dinitroethylene: A Novel Energetic Material with Infinite Layers in Two Dimensions. *Acta Crystallogr. C* **1998**, *54*, 1997−1999.

(2) Lochert, I. J. *FOX-7 - A New Insensitive Explosive*; Australian Aeronautical and Maritime Research Laboratory (AAMRL): Victoria, Australia, 2001; Report no. (DSTO-TR-1238), pp 1−23.

(3) Östmark, H.; Bergman, H.; Bemm, U.; Goede, P.; Holmgren, E.; Johansson, M.; Langlet, A.; Latypov, N.; Pettersson, A.; Pettersson, M. L.; et al. 2,2-Dinitroethene-1,1-Diamine (FOX-7) - Properties, Analysis, and Scale Up. *Proceedings of the 32nd International Annual Conference of the ICT on Energetic Materials*, Vol. *26*, Karlsruhe, Germany, July 4−7, 2001.

(4) Dreger, Z. A.; Gruzdkov, Y. A.; Gupta, Y. M.; Dick, J. J. Shock Wave Induced Decomposition Chemistry of Pentaerythritol Tetranitrate Single Crystals: Time-Resolved Emission Spectroscopy. *J. Phys. Chem. B* **2002**, *106*, 247−256.

(5) Gruzdkov, Y. A.; Dreger, Z. A.; Gupta, Y. M. Experimental and Theoretical Study of Pentaerythritol Tetranitrate Conformers. *J. Phys. Chem. A* **2004**, *108*, 6216−6221.

(6) Hemmi, N.; Dreger, Z. A.; Gruzdkov, Y. A.; Winey, J. M.; Gupta, Y. M. Raman Spectra of Shock Compressed Pentaerythritol Tetranitrate Single Crystals: Anisotropic Response. *J. Phys. Chem. B* **2006**, *110*, 20948−20953.

(7) Dreger, Z. A.; Gupta, Y. M. High Pressure−High Temperature Polymorphism and Decomposition of Pentaerythritol Tetranitrate (PETN). *J. Phys. Chem. A* **2013**, *117*, 5306−5313.

(8) Dreger, Z. A.; Gupta, Y. M. High Pressure Raman Spectroscopy of Single Crystals of Hexahydro-1,3,5-trinitro-1,3,5-triazine (RDX). *J. Phys. Chem. B* **2007**, *111*, 3893−3903.

(9) Patterson, J. E.; Dreger, Z. A.; Gupta, Y. M. Shock Wave-Induced Phase Transition in RDX Single Crystals. *J. Phys. Chem. B* **2007**, *111*, 10897−10904.

(10) Patterson, J. E.; Dreger, Z. A.; Miao, M. S.; Gupta, Y. M. Shock Wave Induced Decomposition of RDX: Time Resolved Spectroscopy. *J. Phys. Chem. A* **2008**, *112*, 7374−7382.

(11) Miao, M. S.; Dreger, Z. A.; Patterson, J. E.; Gupta, Y. M. Shock Wave Induced Decomposition of RDX: Quantum Chemistry Calculations. *J. Phys. Chem. A* **2008**, *112*, 7383−7390.

(12) Miao, M. S.; Dreger, Z. A.; Winey, J. M.; Gupta, Y. M. density Functional Theory Calculations of Pressure Effects on the Vibrational structure of α-RDX. *J. Phys. Chem. A* **2008**, *112*, 12228−12234.

(13) Dreger, Z. A.; Gupta, Y. M. Raman Spectroscopy of High-Pressure-High-Temperature Polymorph of Hexahydro-1,3,5-trinitro-1,3,5-triazine (ε-RDX). *J. Phys. Chem. A* **2010**, *114*, 7038−7047.

(14) Dreger, Z. A.; Gupta, Y. M. Phase Diagram of Hexahydro-1,3,5-trinitro-1,3,5-triazine Crystals at High Pressures and Temperatures. *J. Phys. Chem. A* **2010**, *114*, 8099−8105.

(15) Dreger, Z. A.; Gupta, Y. M. Decomposition of γ-Cyclotrimethylene Trinitramine (γ-RDX): Relevance for Shock Wave Initiation. *J. Phys. Chem. A* **2012**, *116*, 8713−8717.

(16) Dreger, Z. A.; McCluskey, M. D.; Gupta, Y. M. High Pressure-High Temperature Decomposition of γ-Cyclotrimethylene Trinitramine (γ-RDX). *J. Phys. Chem. A* **2012**, *116*, 9680−9688.

(17) Dreger, Z. A.; Tao, Y.; Gupta, Y. M. Polymorphs of 1,1-diamino-2,2-dinitroethene (FOX-7): Isothermal Compression versus Isobaric Heating. *Chem. Phys. Lett.* **2013**, *584*, 83−87.
(18) Dreger, Z. A.; Tao, Y.; Gupta, Y. M. High Pressure Vibrational and Polymorphic Response of 1,1-Diamino-2,2-Dinitroethene (FOX-7) Single Crystals: Raman Spectroscopy. *J. Phys. Chem. A* **2014**, *118*, 5002−5012.
(19) Evers, J.; Klapotke, T. M.; Mayer, P.; Oehlinger, G.; Welch, J. Alpha- and Beta-FOX-7, Polymorphs of a High Energy Density Material, Studied by X-ray Single Crystal and Powder Investigations in the Temperature Range from 200 to 423 K. *Inorg. Chem.* **2006**, *45*, 4996−5007.
(20) Crawford, M. J.; Evers, J.; Gobel, M.; Klapotke, T. M.; Mayer, P.; Oehlinger, G.; Welch, J. M. gamma-FOX-7: Structure of a High Energy Density Material Immediately Prior to Decomposition. *Propellants, Explos., Pyrotech.* **2007**, *32*, 478−495.
(21) Peiris, S. M.; Wong, C. P.; Zerilli, F. J. Equation of State and Structural Changes in Diaminodinitroethylene Under Compression. *J. Chem. Phys.* **2004**, *120*, 8060−8066.
(22) Pravica, M.; Liu, Y.; Robinson, J.; Velisavljevic, N.; Liu, Z.; Galley, M. A High-Pressure Far- and Mid-infrared Study of 1,1-Diamino-2,2-dinitroethylene. *J. Appl. Phys.* **2012**, *111*, 103534−103539.
(23) Bishop, M. M.; Chellappa, R. S.; Pravica, M.; Coe, J.; Liu, Z. X.; Dattlebaum, D.; Vohra, Y.; Velisavljevic, N. 1,1-Diamino-2,2-dinitroethylene Under High Pressure-Temperature. *J. Chem. Phys.* **2012**, *137*, 174304−174308.
(24) Zhao, J. J.; Liu, H. High-Pressure Behavior of Crystalline FOX-7 by Density Functional Theory Calculations. *Comput. Mater. Sci.* **2008**, *42*, 698−703.
(25) Wu, Q.; Zhu, W. H.; Xiao, H. M. DFT Study on Crystalline 1,1-Diamino-2,2-dintroethylene Under High Pressures. *J. Mol. Model.* **2013**, *19*, 4039−4047.
(26) Sorescu, D. C.; Rice, B. M. Theoretical Predictions of Energetic Molecular Crystals at Ambient and Hydrostatic Compression Conditions Using Dispersion Corrections to Conventional Density Functionals (DFT-D). *J. Phys. Chem. C* **2010**, *114*, 6734−6748.
(27) Landerville, A. C.; Conroy, M. W.; Budzevich, M. M.; Lin, Y.; White, C. T.; Oleynik, I. I. Equations of State for Energetic Materials from Density Functional Theory with Van der Waals, Thermal, and Zero-Point Energy Corrections. *Appl. Phys. Lett.* **2010**, *97*, 251908.
(28) Appalakondaiah, S.; Vaitheeswaran, G.; Lebegue, S. Structural, Vibrational, and Quasiparticle Band Structure of 1,1-Diamino-2,2-dinitroethelene from Ab Initio Calculations. *J. Chem. Phys.* **2014**, *140*, 014105.
(29) Sorescu, D. C.; Boatz, J. A.; Thompson, D. L. Classical and Quantum-Mechanical Studies of Crystalline FOX-7 (1,1-Diamino-2,2-dinitroethylene). *J. Phys. Chem. A* **2001**, *105*, 5010−5021.
(30) Clark, S. J.; Segall, M. D.; Pickard, C. J.; Hasnip, P. J.; Probert, M. J.; Refson, K.; Payne, M. C. First Principles Methods using CASTEP. *Z. Kristallogr.* **2005**, *220*, 567−570.
(31) Perdew, J. P.; Burke, K.; Ernzerhof, M. Generalized Gradient Approximation Made Simple. *Phys. Rev. Lett.* **1996**, *77*, 3865−3868.
(32) Grimme, S. Accurate Description of Van der Waals Complexes by Density Functional Theory Including Empirical Corrections. *J. Comput. Chem.* **2004**, *25*, 1463−1473.
(33) Ceperley, D. M.; Alder, B. J. Ground State of the Electron Gas by a Stochastic Method. *Phys. Rev. Lett.* **1980**, *45*, 566−569.
(34) Perdew, J. P.; Zunger, A. Self-interaction Correction to Density-Functional Approximations for Many-Electron Systems. *Phys. Rev. B* **1981**, *23*, 5048−5079.
(35) Monkhorst, H. J.; Pack, J. D. Special Points for Brillouin-Zone Integrations. *Phys. Rev. B* **1976**, *13*, 5188−5192.
(36) Pfrommer, B. G.; Cote, M.; Louie, S. G.; Cohen, M. L. Relaxation of Crystals with the Quasi-Newton Method. *J. Comput. Phys.* **1997**, *131*, 233−240.
(37) Montanari, B.; Harrison, N. M. Lattice Dynamics of TiO2 Rutile: Influence of Gradient Corrections in Density Functional Calculations. *Chem. Phys. Lett.* **2002**, *364*, 528−534.
(38) Krishnakumar, V.; Keresztury, G.; Sundius, T.; Ramasamy, R. Simulation of IR and Raman Spectra Based on Scaled DFT Force Fields: A Case Study of 2-(Methylthio) benzonitrile, with Emphasis on Band Assignment. *J. Mol. Struct.* **2004**, *702*, 9−21.
(39) Bellamy, A. J. In *Struct. Bonding (Berlin, Ger.)*; Mingos, D. M., Ed.; Springer-Verlag: Berlin, 2007; Vol. *125*, pp 1−33.